Mechanism Of Fatigue Crack Initiation Of 316N Weldment Under The Influence E Of Cyclic Stress Amplitude In A Corrosive Environment

A. Poonguzhali[1*,3], M. G. Pujar[1], and U. Kamachi Mudali[2,3]
[1]Corrosion Science and Technology Division, MMG, IGCAR, Kalpakkam, India [1]Corrosion Science and Technology Division, MMG, IGCAR, Kalpakkam, India [2]Materials Chemistry and Metal Fuel Cycle Group, IGCAR, Kalpakkam, India [3]Homi Bhabha National Institute, Mumbai
* apoongs@igcar.gov.in

Abstract:

Total fatigue life of the material consists of initiation and propagation of fatigue cracks. Several approaches are available in literature for prediction of fatigue life and crack growth phenomena. In this connection an attempts was made to understand and estimate the fatigue initiation time using the compliance based approach. The corrosion fatigue behavior of 316N weldments was investigated with a view to know the effect of the mean stress on the damage characteristics. It was found that the S-N curve of the fatigue life vs. the mean stress showed a specific bilinear Basquin relationship. The process of formation, blunting and resharpening of crack delays the crack propagation at low stress amplitudes whereas, at high stress amplitudes the barriers to dislocation motion is overcome thereby crack initiation becomes easier. At low stress amplitude, the deformation microstructure consists mainly of planar slip dislocation structure and at high stress amplitudes, planar multiple slip dislocations and deformation induced persistant luder's band (PLBs) govern the cyclic behavior. A correlation between microstructural changes and the corresponding susceptibility of the 316N SS weldment in as-welded condition towards environmental cracking in boiling acidified aqueous solution has been presented.

Keywords: Corrosion fatigue, Nitrogen, Stainless steel, Crack initiation and Deformation

1. Introduction

Cyclic loading on a structural component can result due to changes in mechanical and thermal loading as the system changes from one load set to other load set with respect to pressure, temperature, moment and force. Environmentally assisted fracture is a complex process because of the localized nature of the material-stress-environment interaction and the varied mechanisms by which an environment can affect the material behavior [1]. The fatigue failure life consists of two stages namely the crack initiation and the crack growth periods. A number of crack initiation mechanisms have been suggested which include competition between pit growth and short crack growth [2], preferential dissolution of plastically deformed material [3], local rupture of the passive film by persistent slip bands (PSB) and hydrogen embrittlement in the cathodic domain [4]. During corrosion fatigue of passive metals the cyclic strain can induce a breakdown of the surface film which enhances local electro-chemical reactions depending on the potential and the chemistry of the system. Thus, crack initiation mechanisms are generally studied from surface dissolution effects which are related to the competition between the kinetics of depassivation as well as repassivation [5-7]. Thus, the surface dissolution processes of passive metals, are partly dependent on the mechanical parameters which govern the emergence of slip steps as well as the depassivation kinetics [8] resulting in the breakdown of the film. The purpose of the present study is to understand the initiation

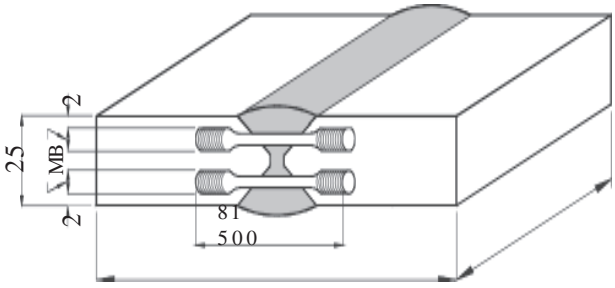
Table 1: Chemical composition of AISI type 316LN SS and 316N SS weld metal, wt.%

Wt.%	C	Cr	Ni	Mo	Mn	Si	N	S	P
Type 316LN SS	0.025	18.16	11.9	2.4	1.6	0.28	0.086	0.01	0.044
316N Weld Metal	0.061	19.7	10.7	2.1	1.8	0.7	0.11	0.01	0.022

mechanism in 316N austenitic SS weldment during tension-tension corrosion fatigue loaded in the high cycle fatigue (HCF) domain between 10^4 and 10^6 cycles under load control mode. Hence, an attempt was made to understand and estimate the fatigue initiation life using the compliance based approach.

2. Experimental

The chemical composition of the steel and the electrode is shown in Table1. The 316LN SS weldpads of 500 x 250 x 25 mm^3 size were fabricated by employing multi-pass shielded metal arc welding process using a double-V-groove joint configuration. The weld pads were qualified by radiographic examination for their soundness. Round tensile specimens with 15 mm gauge length and 4 mm gauge diameter were used for tests as per ASTM E8. Fig. 1 shows the schematic of the weld pad and Table 2 gives the details of the welding parameters. As-welded specimen is electrolytically etched at 2 V in 10% oxalic acid for 15 s to reveal the 6-ferrite. Corrosion fatigue tests were carried out at a frequency (y) of 0.1 Hz using a servo hydraulic system of 25 kN capacity under axial loading in load controlled mode in boiling aqueous solution of 5 M NaCl + 0.15 M Na_2SO_4 + 2.5 ml/l HCl (b.p = 381.5 K, pH = 1.3) at different mean stress values and R-ratio of 0.5. The entire specimen except the gauge section was exposed to the boiling corrosive solution and the electrochemical parameters were monitored using a potentiostat which was connected with the specimen externally. Weldments in as-desposited condition were studied at different mean stress values. Number of cycles to total failure was used as the assessment criterion for determining the susceptibility to corrosion fatigue. After the tests, the fracture surfaces were observed using a scanning electron microscope (SEM) to investigate the fracture surface.



Location of specimens

Figure 1: A schematic of the weld joint configuration used in the present study.

Table 2: Weld pad details

Joint design	Arc Voltage, V	Arc Current, A	Torch speed, mm/min	No. of passes
'K' Joint	10 - 15	110 - 130	95 - 110	6

3. Results and Discussion

The mode of solidification for the weld metals with the Creq/Nieq ratios within the range of 1.25–1.48 is austeno-ferritic (AF) [9]. The microstructure of the as-deposited weld metal showed a discontinuous network of vermicular ferrite as seen in Fig. 2. ferritoscope measurements on the as-deposited weld metal showed an average 6-ferrite content of 5 FN. The fatigue life of specimen was obtained in terms of number of cycles to failure at variable amplitude loading. Stress amplitude versus fatigue life is plotted

to view the significant difference of fatigue life at higher stress compared to the lower stress with stress-based approach for fatigue analysis and design as seen in Fig. 3. The relation is given by:

$$bo/2=o_f' (2N_f)^b \quad (1)$$

Where o_f' is the fatigue strength coefficient, and N_f is the fatigue life. The slope corresponds to the fatigue strength exponent or Basquin exponent 'b' in the Basquin relation. The exponent 'b' represents the sensitivity of fatigue life to stress amplitude, i.e., a lower absolute value of b reflects a higher sensitivity of fatigue life to stress amplitude. The Basquin exponent 'b' in the range of high stress amplitudes has a lower absolute value of 0.02 as compared to the value of 0.26 in the range of low Oo/2, implying a notable change of fatigue damage mechanism on varying the stress amplitude from low to high levels. A transition occurs as shown in Eq. (1) resulting in a bi-linear relationship due to change in the plastic

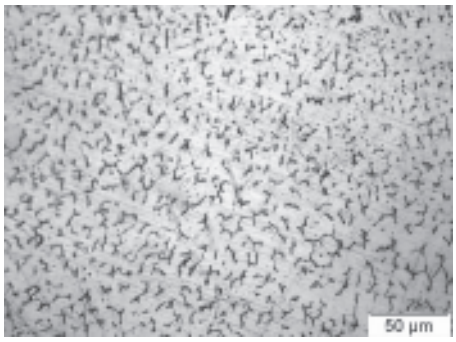


Figure 2: As welded joint showing 6-ferrite with vermicular morphology.

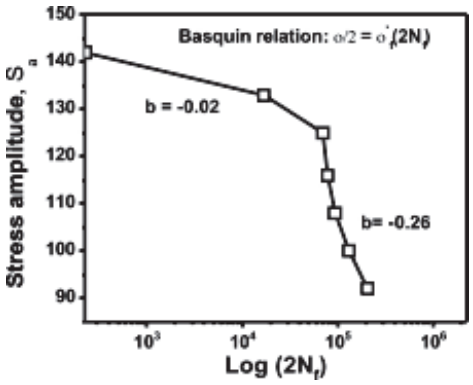
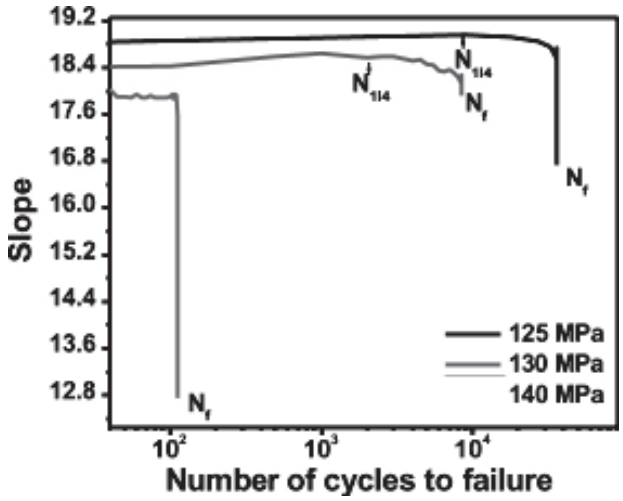


Figure 3: S- N curve between stress amplitude (bo/2) and fatigue life (N_f)

deformation behavior through the work-hardening characteristics, fracture morphology at different strain amplitudes and environmentally assisted fatigue degradation [10]. The slope of the hysteresis loop is calculated at the regular intervals of the loading. The slope of the loop for higher stress amplitude (140 MPa) does not show any variation till failure. At stress amplitudes 130 and 125 MPa, it was observed in Fig. 4a that the slope of the hysteresis loop decreases marginally as the cycle reaches one-fourth the life of the specimen ($N_{1/4}$). At lower stress amplitudes, hardening occurs till 75% of the total life of the specimen which results in drastic decrease in slope. Weld metals exhibited initial hardening followed by a gradual softening regime, at low stress amplitudes as seen Fig. 4b. The amount of damage resulting from each of hysteresis loop depends on the damage parameter [11], D_E, defined as

$$D_E = 1 - (E/E_0) \quad (2)$$

where E is the secant modulus for a given cycle of stress-strain curve and E_0 is the elastic modulus. The damage parameter calculated for higher stress amplitudes indicates that 25% of the life is spent for the crack initiation at high stress amplitudes in corrosive environment and for lower stress amplitude, 75% of life is spent for the micro crack initiation as seen in Fig.5(a &b). The SEM observation shows that the plastic deformation associated with fatigue testing accelerates the dissolution of slip steps within the slip bands at higher stress amplitudes as seen in Fig. 6a. Figure 6 (b & c) revealed that most of the fatigue cracks regularly nucleated at many stable pits on the surface of the specimens in all the fatigue ranges and unstable fracture mode was explored in final stages called the rupture zone [12]. At low (Oo/2), the deformation microstructures consist mainly of planar slip dislocation structure [13] and at high (Oo/2), planar multiple slip of dislocations and deformation induced persistant luder's band (PLBs) [14] govern the cyclic behaviour as shown in Fig, 7 (a & b). The multiple slip mode with dislocations intersects especially in the area near grain boundaries, finally leading to the formation of dislocation networks



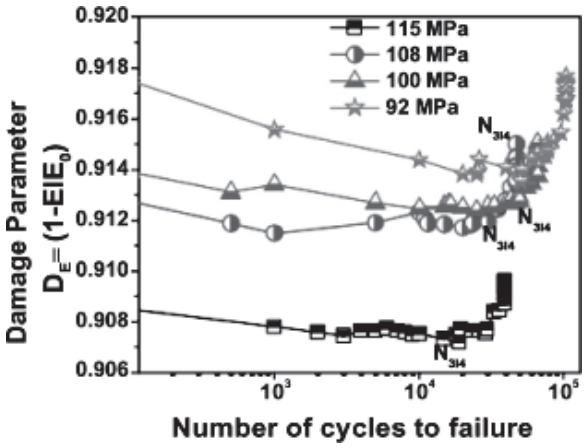
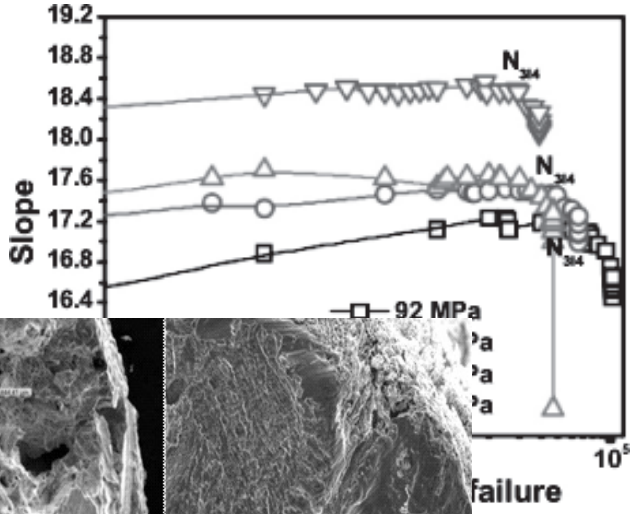
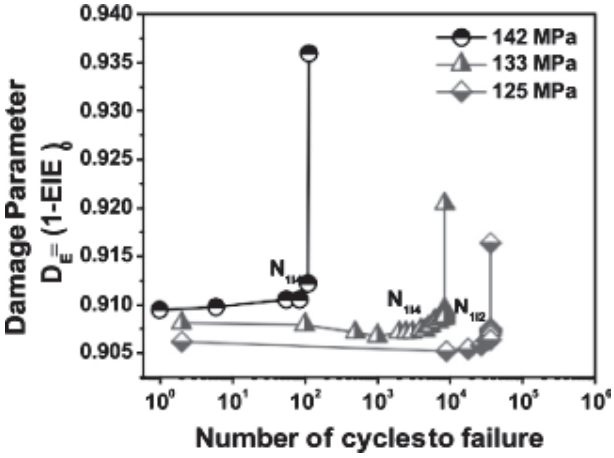


Figure 5(a & b): Damage parameter from slope of stress-strain hysteresis loop



op vs N_f for higher and lower stress amplitudes.



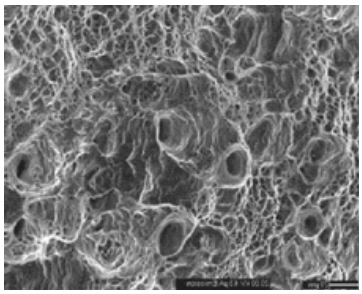
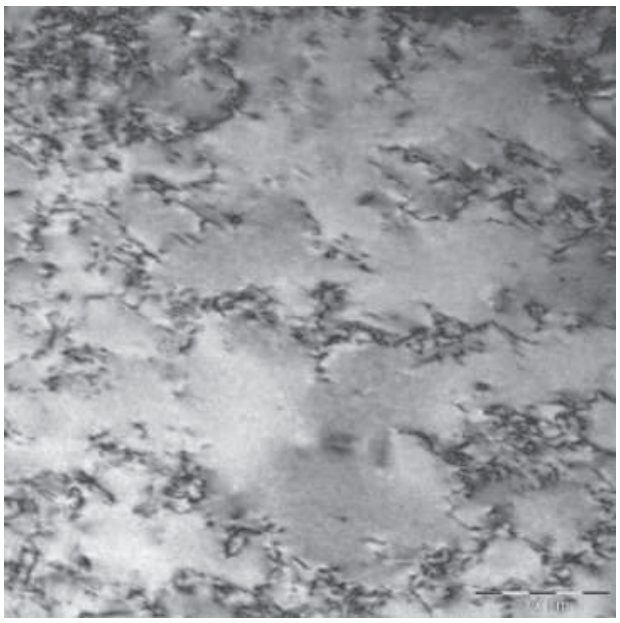


Figure 6 (a, b & c): Fractographs of surface deformation and damage features at a) high stress amplitude, b) low stress amplitude and c) dimpled features during rupture zone.

4. Conclusions

The number of cycles to failure decreased with increasing mean stress for 316N weldment. It was observed that about 25% to 75% of life is spent for initiation of the micro cracks at low as well as high stress amplitudes. The S-N curve shows a specific bilinear Basquin relationship. With increasing stress amplitude, the damage features change gradually from slip cracking into transgranular cracking. The deformation

microstructures consist mainly of planar slip dislocation structure and planar multiple slip of dislocations and deformation induced PLBs govern the cyclic behaviour at low and high stress amplitudes.



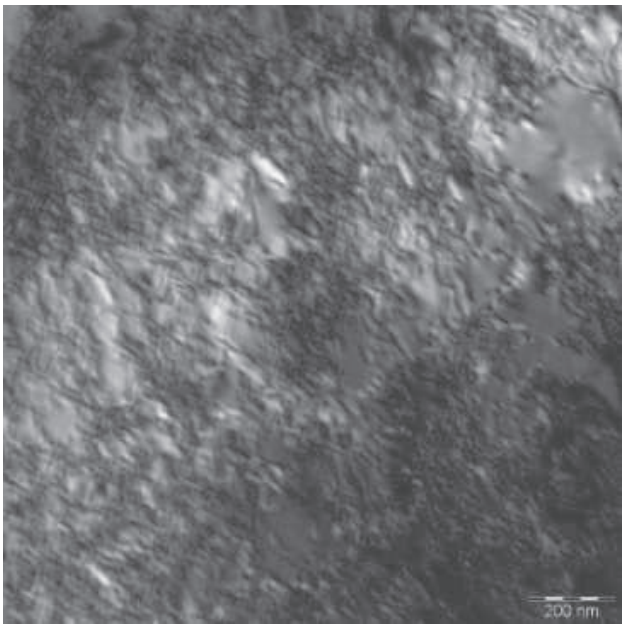


Figure 7: TEM images of dislocation structures of 316LN weldment cycled a) at low bo/2 = 300 MPa and b) at high bo/2 = 400MPa

5. References

1. A. Poonguzhali, M.G. Pujar, C. Mallika and U Kamachi Mudali, CEST, 2016.22, 1- 8.
2. Kondo Y, Corrosion, 1979.45,7–11.
3. Xu S, Wu XQ, Han EH, Ke W, Katada Y, Mat Sci Eng A, 2008.490, 16–25.
4. Mohamed El Maya, Thierry Palin-Luc, Nicolas Saintier, Olivier Devos, International Journal of Fatigue, 2013.47, 330–339.
5. T. Pyle, V. Rollins and T. Howard, J. Electrochem. Soc., 1975.11, 1445- .
6. H. N. Hahn and D. J. Duquette, Acta Metall., 1978.26, 279 - .
7. T. Magnin and A. Desestret, Mem. Sci. Rev. Metall.,1983.11, 641-.
8. T. Magninand L. Coudreuse, Materials Science and Engineering,1985.72, 125-134
9. K. Rajasekhar, C.S. Harendranath, R. Raman, S.D. Kulkarni, Mater. Characterization, 1997. 38, 53-.
10. Mediratta, S.R.; Ramaswamy, V.; and Rao, P.R.,Scr. Metall., 1986.20, 555-558.
11. Z.R. Xu, K.K. Chawla, A. Wolfenden, A. Neuman, G.M. Liggett, N. Chawla, Materials Science and Engineering A, 1995.203A, 75-80.
12. K. A. Mohammad, Aidy Ali, B. B. Sahariand S. Abdullah, Materials Science and Engineering, 2012.36,
13. C.W. Shao, F. Shi, X.W. Li, Metall. Mater. Trans. A, 2015.46, 1610.
14. X.W. Li, N. Peng, X.M. Wu, Z.G. Wang, Metall. Mater. Trans. A, 2014.45, 3835.